Journal of Alloys and Compounds 509 (2011) 6532–6538

Contents lists available at ScienceDirect

Journal of Alloys and Compounds

journal homepage: www.elsevier.com/locate/jallcom

Selective dry oxidation of the ordered Pt–11.1 at.% V alloy surface evidenced by *in situ* temperature-controlled X-ray diffraction

Gwenaël Corbel[a,*], Miroslava Topić[b], Alain Gibaud[c], Candace I. Lang[d]

[a] Laboratoire des Oxydes et Fluorures, UMR-6010 CNRS, Université du Maine, Avenue Olivier Messiaen, 72085 Le Mans cedex 9, France
[b] iThemba Laboratory for Accelerator Based Sciences, Materials Research Department, PO Box 722, Somerset West 7129, South Africa
[c] Laboratoire de Physique de l'Etat Condensé, UMR-6087 CNRS, Université du Maine, Avenue Olivier Messiaen, 72085 Le Mans cedex 9, France
[d] Centre for Materials Engineering, Mechanical Engineering Department, University of Cape Town, Private Bag X3, 7701 Rondebosch, South Africa

ARTICLE INFO

Article history:
Received 28 January 2011
Received in revised form 8 March 2011
Accepted 13 March 2011
Available online 21 March 2011

Keywords:
Metal and alloys
X-ray diffraction (XRD)
Order–disorder transition
Metastability
Selective oxidation
Segregation
Vanadium oxide
Platinum

ABSTRACT

A temperature-controlled X-ray diffraction study of the cold-rolled Pt–11.1 at.% V alloy was undertaken to gain better insight into the incomplete transformation of the metastable cubic disordered phase into the tetragonal ordered Pt_8V phase, earlier reported by Nxumalo and Lang [11]. This study has revealed a complex behaviour of the alloy when is annealed in primary vacuum. Upon heating above 450 °C, an ordering of vanadium atoms in the Pt–11.1 at.% V alloy leads to the appearance of a tetragonal Pt_8V phase. Concomitantly, vanadium atoms at the surface of the ordered alloy are slowly oxidized into V_2O_3 Corundum type phase by the low oxygen partial pressure existing in primary vacuum. This segregation of vanadium oxide onto the surface depleting the subsurface region in vanadium, an almost pure Pt cubic phase grows at the V_2O_3-ordered Pt_8V alloy interface with increasing the temperature. This investigation also shows that an external selective oxidation of the cold-rolled Pt–11.1 at.% V alloy takes place when is annealed in flowing argon atmosphere.

1. Introduction

Platinum is a precious metal, which is widely used in variety of applications. Platinum and platinum alloys are important constituents of catalysts (chemical reaction, automotive exhaust gas cleaning, electrodes of proton exchange membrane fuel cells), temperature sensor materials, high temperature and corrosion resistant structural parts, electronic and optical devices. However, it is a very ductile material in its pure state and thus, it has limited applications when mechanical properties are concerned. In general, the mechanical strength and hardness of platinum can be enhanced by mechanical cold working, by alloying with other metals such as chromium, copper, ruthenium or vanadium, by irradiation using protons or neutrons or by the combination of these processes [1–5].

Alloying platinum with an element of group IVA, VA, and VIA is well documented in the literature. Increase the solute content in platinum alloys can give rise to long-range ordered structure either thermodynamically stable or exhibiting order/disorder phase transition upon heating [6]. Among long-range ordered structures, several Pt–11.1 at.% *A* alloys (*A* = Ti, Zr, V, Cr [7–13]) crystallize in a body centred tetragonal (BCT) Pt_8A super-structure (space group *I*4/*mmm* (no. 139)) derived from the single face cubic centred (FCC) structure of pure platinum by a 45° rotation of the unit cell with the following cell parameters $a_{BCT} \approx 3/2 \times \sqrt{2} \times a_{FCC} \approx 8.31$ Å and $c_{BCT} \approx a_{FCC} \approx 3.89$ Å. This ordered crystal structure was determined for the first time in 1965 by Pietrokowsky [7] for the binary Pt_8Ti alloy. Fig. 1 shows the relationship between the single cubic structure of Pt (dashed line) and the ordered tetragonal super-structure of Pt_8Ti (solid line). In this Pt_8Ti phase, Ti atoms are ordered and located at the centre and corners of the tetragonal super-cell. This structural type is also found in nickel- or palladium-based alloys Ni_8X (*X* = V, Nb, Ta [14–16]), Pd_8T (*T* = Mo, W [17–20]).

In a previous paper, we have studied the effect of alloying platinum with vanadium for compositions ranging from 1 at.% to 11.1 at.%V [21]. When fabricated from the melt and cold-rolled, all compositions in this range of concentration are pure and exhibit at room temperature the face cubic centred crystal structure of the platinum metal. Along this $Pt_{1-x}V_x$ series, the linear reduction of the cubic lattice parameter a_{FCC} with increasing the vanadium content *x* reflects that V atom ($r_V = 0.1311$ nm) is smaller than Pt atom ($r_{Pt} = 0.1389$ nm) thus confirming that the partial

* Corresponding author at: Laboratoire des Oxydes et Fluorures, UMR-6010 CNRS, Institut de Recherche en Ingénierie Moléculaire et Matériaux Fonctionnels, IRIM2F, FR CNRS 2575. Université du Maine, Avenue Olivier Messiaen, 72085 Le Mans Cedex 9, France. Tel.: +33 0 2 43 83 26 48; fax: +33 0 2 43 83 35 06.
E-mail address: gwenael.corbel@univ-lemans.fr (G. Corbel).

0925-8388/$ – see front matter © 2011 Elsevier B.V. All rights reserved.
doi:10.1016/j.jallcom.2011.03.079

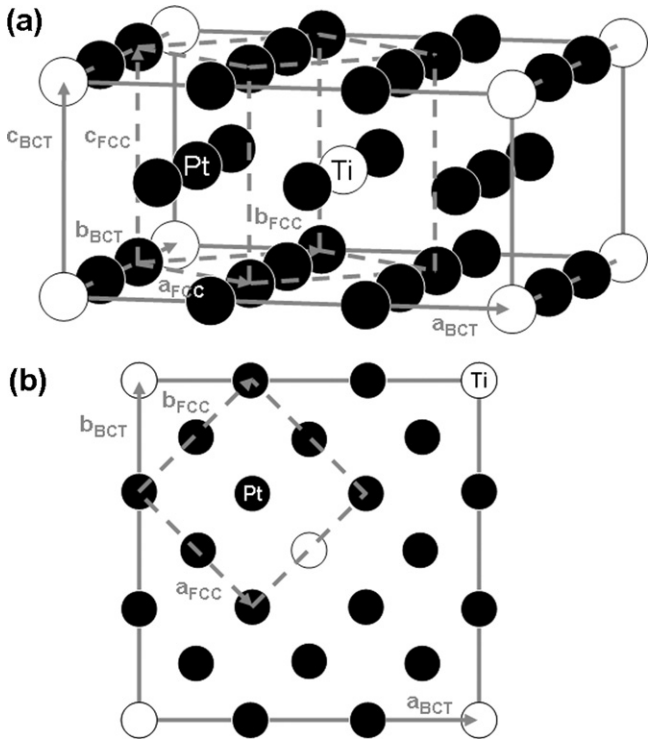

Fig. 1. Illustrations of the change from the single cubic structure of Pt (FCC, space group *Fm*-3*m* no. 225) to the ordered tetragonal superstructure (BCT) of Pt_8Ti with Pt-1 (1/3, 1/3, 0), Pt-2 (1/3, 0, 0) and Ti (0,0,0) in special atomic positions of the space group *I*4/*mmm* (no. 139).

substitution of platinum by vanadium is effective. Schryvers et al. [9] and Schryvers and Amelinckx [10] have shown that the tetragonal Pt_8V phase can be obtained at room temperature when the Pt–11.1 at.% V alloy is annealed for 2 days at 700 °C. Moreover, Nxumalo and Lang [11] have recently probed the thermodynamic stability of the cubic disordered form of the Pt–11.1 at.% V alloy by re-annealing the cold-rolled specimens in argon for 3 h and quenching them into water from 200, 300, 400, 500, 600, 700, 800, 900 and 1000 °C. The characterization by transmission electron microscopy (TEM) of the samples annealed in the temperature range 300–800 °C has revealed that only a fraction of the cubic disordered phase is converted into a tetragonal ordered Pt_8V phase. This type of disorder/order transition is reminiscent of the diffusionless phase transformation of austenite into martensite described by Bain [22] (continuous change of the single face cubic centred unit cell into a tetragonal unit cell). However, the ordering of vanadium in the cold-rolled Pt–11.1 at.% V alloy remains incomplete even after long annealing times at 400 °C (2736 h) or at a higher temperature 600 °C (720 h). A better understanding and control of this incomplete transformation is of considerable importance to increase the benefit effect of this partial vanadium ordering on the hardness of the Pt–11.1 at.% V alloy, reported by Nxumalo et al. [13]. Since a limited electron transparent area of the sample is analysed by transmission electron microscopy which might not be representative of the whole of the sample, *in situ* temperature-controlled X-ray diffraction has been used in the current investigation to provide key information in understanding the incomplete ordering of vanadium in the cold-rolled Pt–11.1 at.% V alloy.

2. Experimental

Button of Pt–11.1 at.% V alloy was produced by arc melting of pure platinum (99.99 wt.%) and vanadium (99.8 wt.% purity) in stoichiometric amount. The button was re-melted under argon atmosphere at 900 °C for 8 h to promote homogeneity before casting. The melt was afterwards cooled down at a rate of 10 °C/min and the button was cold-rolled. Due to extremely high rate of hardening making difficult the multi-rolling process, the sample was subjected to re-annealing at 900 °C for 8 h under vacuum conditions (1.10^{-4} mbar) after every 20th rolling pass. A total of 100 rolling pass was needed to obtain a sample of 1 mm in thickness. Finally, a 1 cm × 1 cm square specimen was cut out and was then mechanically polished according to the process: firstly with silicon carbide papers (from 80 to 1200 grit) followed by successive polishes with diamond pastes (grit particles of 3 μm, 1 μm and 0.25 μm in size) and alumina suspension.

The thermal stability of the Pt–11.1 at.% V alloy was studied by temperature-controlled X-ray diffraction on the top surface of the specimen in a dynamic primary vacuum atmosphere of about 10^{-2} mbar. In a first stage, primary vacuum atmosphere was preferred to flowing argon one since argon gas has a low thermal conductivity and a high X-rays mass attenuation coefficient. The experiments were performed on a PANalytical θ/θ Bragg-Brentano X'pert MPD PRO diffractometer ($CuK\alpha_{1+2}$ radiations) equipped with the X'celerator multi-elements detector and a HTK 1200 Anton Paar chamber. Data collection was carried out in the (12.5–90°) scattering angle range with a 0.0167° step over 125 min at RT, 103 °C, 209 °C and every 25 °C from 316 to 846 °C (heating/cooling rates of 10 °C/min, temperature stabilisation for 20 min with temperature correction after calibration [23]). The program FullProf [24] was used for Le Bail's refinements. The effect of isothermal annealing at 600 °C (corrected temperature, heating rate of 30 °C/min) in flowing argon atmosphere was carried out by *in situ* X-ray diffraction. The raw sample was continuously scanned in terms of successive periods of 20 min for 800 min. Each scan was performed in the (28.5–40.5°) scattering angle range with a 0.0167° step.

A Hitachi S2300 scanning electron microscope (SEM) coupled to a Link/Oxford energy dispersive X-ray spectrometer (EDX) was used to determine the chemical composition on 10 randomly selected point locations on the surface of the alloy. In addition, EDX cartographies were recorded in order to check the homogeneous distribution of elements on the surface.

3. Results and discussion

In the (12.5–34.5°) scattering angle range of temperature-controlled X-ray diffraction patterns (Fig. 2a), seven extra diffraction peaks emerged, as the temperature increases up to 713 °C, from the weak undulations of the background detected at around 300 °C. Five of them can be successfully indexed in the *I*4/*mmm* super-cell, proposed by Pietrokowsky [7] for Pt_8Ti. The vanadium ordering in Pt–11.1 at.% V alloy is then similar to that observed in Pt_8Ti, as Schryvers et al. [9] and Schryvers and Amelinckx [10] showed by transmission electron microscopy.

It must be pointed out that Nxumalo and Lang [11] have reported that the ordered tetragonal Pt_8V phase exists in the temperature range starting from 300 to 810 °C while the alloy has the cubic disordered structure above 810 °C. However, a different thermal behaviour is highlighted in our *in situ* study. As shown in Fig. 3, the intensity of the $(2\,2\,0)_{BCT}$ reflection first strongly increases as the temperature increases up to 633 °C and falls down above this temperature while the full width at half maximum (FWHM) exponentially decreases in this whole thermal range. Note that, all of superstructure peaks belonging to the ordered Pt_8V structure have completely disappeared above 713 °C. In order to explain such a discrepancy with Nxumalo et al. study, our attention was focussed on the 11 additional diffraction lines remaining non-indexed in the *I*4/*mmm* super-cell associated to the ordered BCT phase. A strong rise in their intensity as the temperature increases above 713 °C takes place only when the BCT superstructure peaks have completely disappeared. An attempt to index these extra diffraction lines was performed by using the program TREOR-90 [25]. A solution with a trigonal/rhombohedral symmetry and the cell parameters $a = 5.034(2)$ $c = 13.951(4)$ (hexagonal axes) was obtained (figures of merit $M(1\,1) = 31$ and $F(1\,1) = 10$ [26]). A good match with V_2O_3 corundum type phase (space group no. 167 *R*-3*c*, PDF 01-070-8656 [27]) is found and the two peaks at $2\theta \approx 24°$ and $2\theta \approx 32.75°$ in Fig. 2a are indexed as the $(0\,1\,2)$ and $(1\,0\,4)$ reflections, respectively. This result is in good agreement with the grey–black colour of the whole surface of the sample after temperature-controlled X-ray diffraction experiment. It is known that vanadium metal can be easily oxidized in air above 660 °C via the lower oxides to V_2O_5 [28] but this oxidation can also take place

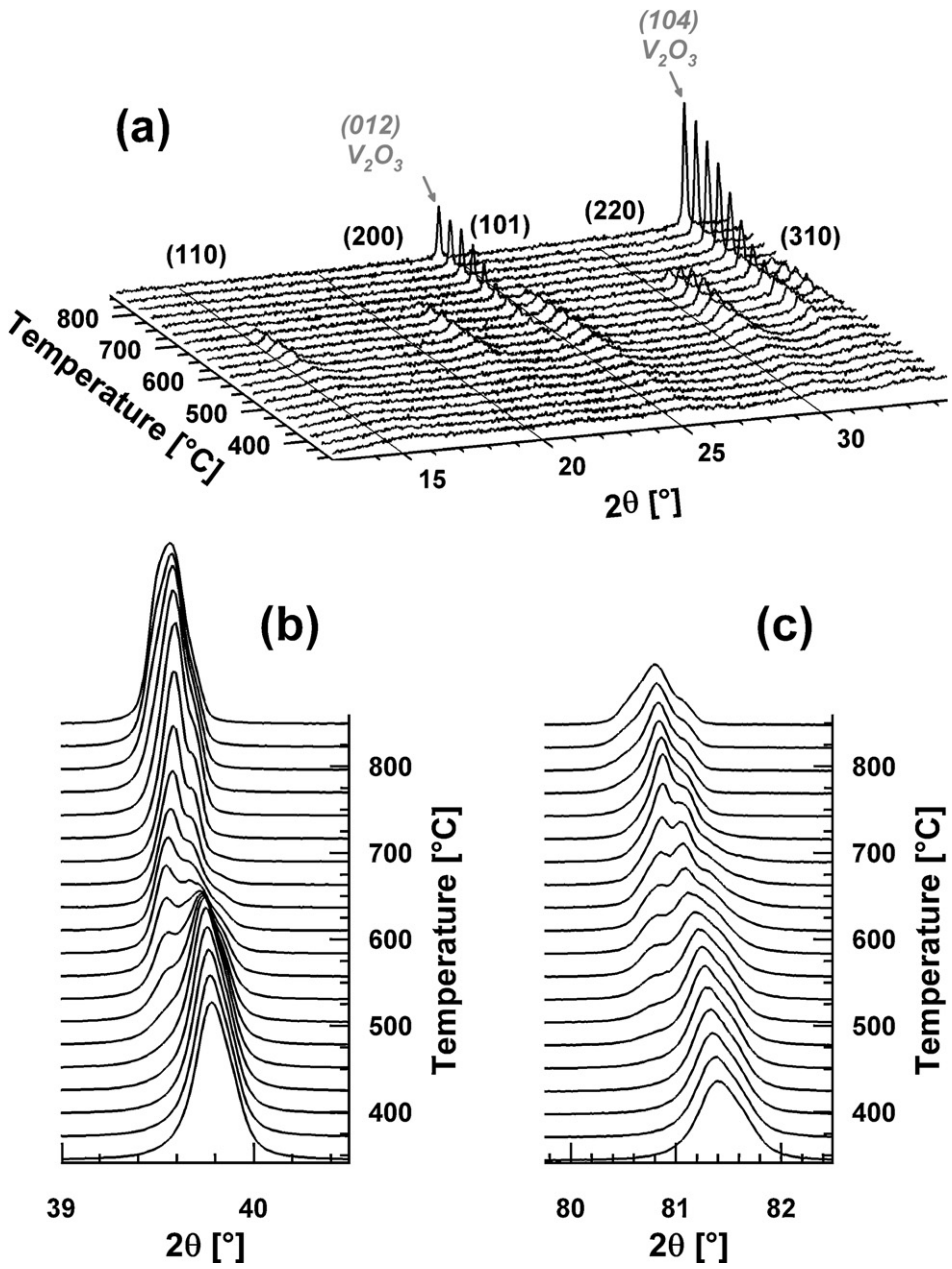

Fig. 2. Evolution upon heating of the X-ray diffraction pattern of Pt–11.1 at.% V alloy showing the growth of tetragonal ordered phase (BCT) in the range 448–713 °C from the cubic metastable-disordered phase (FCC) and its sudden disappearance above 713 °C due to the oxidation of vanadium into V_2O_3. (a) Superstructure peaks at low scattering angles of the tetragonal (BCT) phase, (b) Overlapping of the $(1\,1\,1)_{FCC}$ cubic peak and $(3\,0\,1)_{BCT}$ tetragonal peak and (c) Overlapping of the $(3\,1\,1)_{FCC}$ cubic peak and the $(6\,3\,1)_{BCT}$ + $(3\,0\,3)_{BCT}$ tetragonal peaks.

at ambient temperature by long exposure to low O_2 partial pressure [29]. In the current study, this partial oxidation of vanadium seems to occur above 554 °C under primary vacuum conditions.

Then, only temperature-controlled diffraction patterns collected at a temperature lower than 554 °C were thoroughly analysed. It is worth noting that a strong preferred orientation effect arising from the severe mechanical work is observed on all diffraction patterns collected. All attempts to model these strain effects in Rietveld refinements remained unsatisfactory. In that way, only Le Bail fits of diffractograms were carried out (Fig. 4). Below 448 °C, the diffraction patterns can be satisfactorily fitted with a single cubic disordered Pt–11.1 at.% V phase (space group *Fm*-3*m* no. 225). The temperature dependences of cell parameters and cell volumes are reported in Fig. 5 (solid circles), together with those of pure cold-rolled Pt sample (open squares) for reference. In Fig. 5, the reduction in cell dimension of the cubic Pt–11.1 at.% V phase when compared to that of pure Pt reflects that vanadium atom is much smaller in size than platinum. However, both Pt and disordered cubic Pt–11.1 at.% V phases exhibit a similar linear thermal expansion with an average thermal expansion coefficient $\alpha_{RT-625\,^\circ C} = 10.2 \times 10^{-6}\,^\circ C^{-1}$ and $\alpha_{RT-425\,^\circ C} = 11.1 \times 10^{-6}\,^\circ C^{-1}$, respectively. At 448 °C, the peak shape of the disordered cubic Pt–11.1 at.% V phase changes as shown in Fig. 2b and c. In the (79.75–82.5°) range, two shoulders appear on both sides of the strongest peak. If the former at lower scattering angle remains weak, the second is relatively intense at higher scattering angle (Fig. 2c). The most intense shoulder was satisfactorily modelled in Le Bail fit of the diffraction pattern with a tetragonal super-cell thus confirming the occurrence of the Bain transformation (Fig. 4). The temperature dependences of cell parameters and volume for

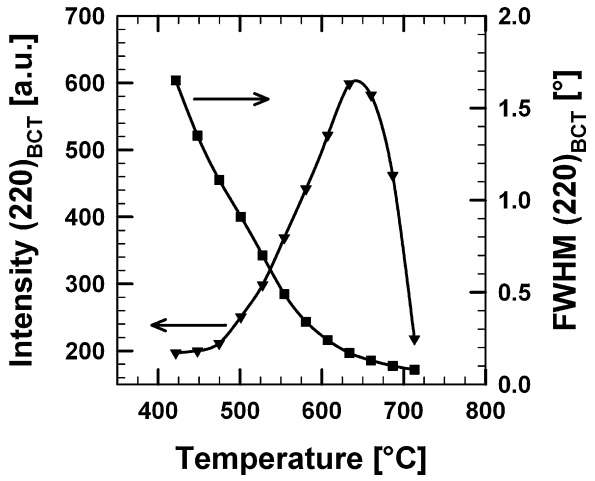

Fig. 3. Temperature dependences of the peak intensity (triangles) and the full width at half maximum (FWHM, squares) for the $(2\,2\,0)_{BCT}$ bragg reflection.

the ordered tetragonal phase are reported in Fig. 5 (triangles). In the Bain transformation, the c_{BCT}-axis of body centred tetragonal super-cell of the ordered phase corresponds to the c_{FCC}-axis of the single face cubic centred cell of the parent phase as shown in Fig. 1. This explains why the thermal evolution of the c_{BCT} cell parameter as the temperature increases above the disorder/order phase transition temperature is in keeping with the linear thermal expansion of the a_{FCC} cell parameter below this temperature.

It is important to note, however, that the weakest peak at $2\theta \approx 80.8^\circ$ continuously grows in intensity with increasing the temperature. The coexistence of ordered and disordered domains in initially cold worked Pt–11.1 at.% V and later annealed in argon at 400 °C for 2736 h was earlier shown by Nxumalo and Lang [11] thanks to transmission electron microscopy (after ion polishing of the surface). Then, Le Bail fits of the diffraction patterns with a secondary cubic phase were attempted and successfully performed, as shown in Fig. 4. The temperature dependences of cell parameters and volume for this secondary cubic phase in the range 448–554 °C are also displayed in Fig. 5 (solid squares). One can note that this phase has a cubic cell parameter very close to that of a pure Pt phase. This shows that an almost complete depletion of vanadium from the Pt_8V phase occurs even at temperature lower than 554 °C. Nevertheless, no trace of a ternary phase containing the exsolved vanadium is detected in X-ray diffraction patterns collected in the temperature range 448–554 °C. This suggests that the weight fraction of vanadium exsolved from the alloy in this temperature range remains too small to be detected by diffraction. Attempts to determine the weight fractions of the cubic Pt phase and of the tetragonal Pt_8V phase using the Rietveld method failed due mainly to the unsatisfactory modelling of the strong preferred orientation effect and to the strong overlap of the Bragg reflections of both phases. At 554 °C, extra diffraction peaks ascribed to the sesquioxide V_2O_3 starts emerging from the background. The strong rise in their intensity as the temperature increases above 554 °C indicates that a layer of V_2O_3 grows onto the surface of the Pt–11.1 at.% V alloy thus progressively depleting the subsurface region in vanadium. This is supported by the concomitant intensity increase of

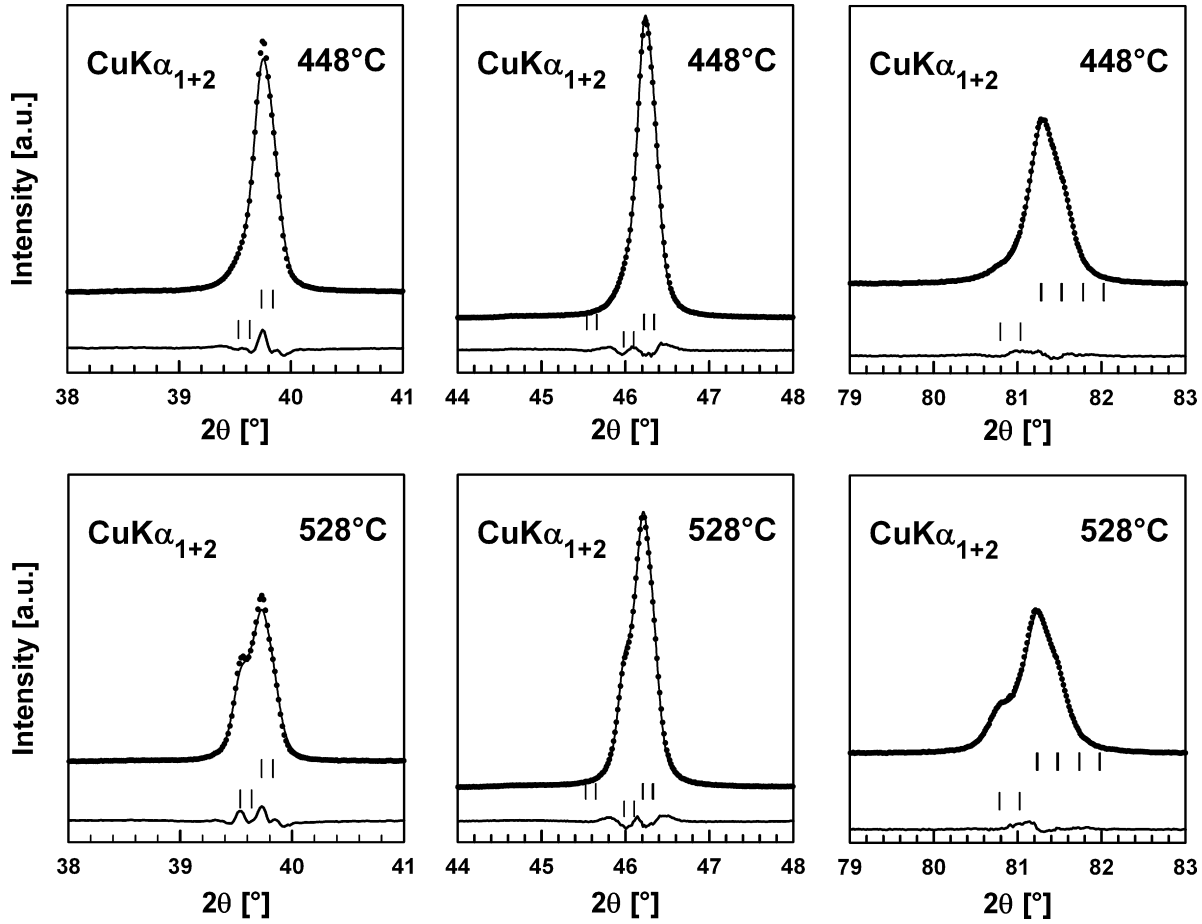

Fig. 4. Observed (solid circles), Le Bail's fitted (lines), and difference (below) patterns showing the coexistence of ordered tetragonal and disordered cubic phases. Vertical markers give Bragg peak positions of space groups *I*4/*mmm* (no. 139) (top) and *Fm*-3*m* (no. 225) (bottom), respectively.

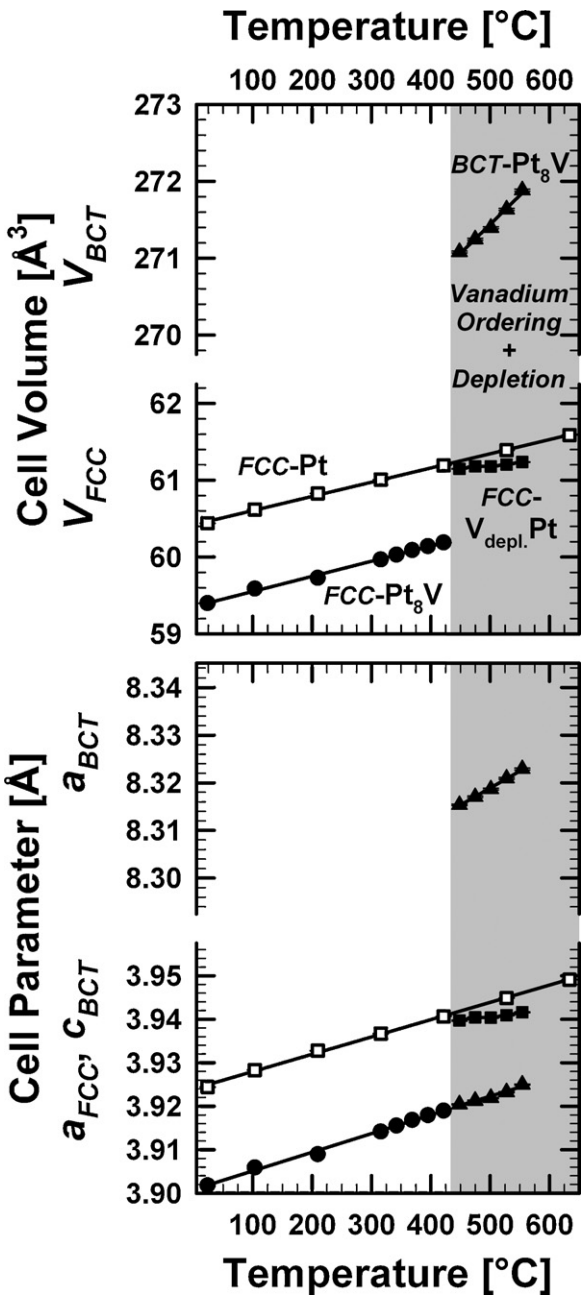

Fig. 5. Temperature dependences of unit cell parameters and volumes of the FCC-Pt_8V (solid circles), BCT-Pt_8V (triangles), vanadium-depleted Pt (solid squares) phases determined from Le Bail's fit of temperature-controlled X-ray diffraction patterns (see details in the text). The thermal expansion of pure FCC-Pt sample is added (open squares) for reference. Errors bars are approximately the size of the symbols.

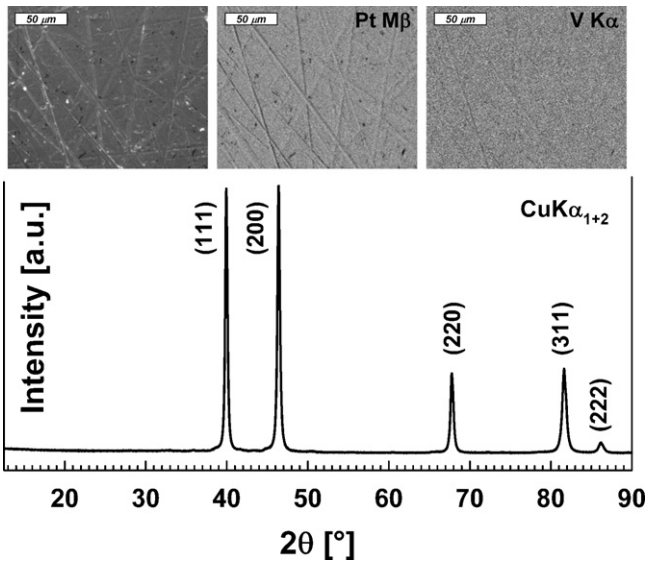

Fig. 6. SEM image, EDX cartographies and X-ray diffraction pattern (peak indexation of the cubic metastable form) collected at room temperature after in-depth polishing (≈−0.04 mm) of the Pt–11.1 at.% V alloy annealed at 846 °C and cooled down at 10 °C/min in primary vacuum.

diffraction peaks ascribed to the vanadium-depleted (almost pure) Pt cubic phase (Fig. 2b and c). In order to confirm that this vanadium depletion takes place only near the surface rather than in the bulk of the sample, the previous Pt–11.1 at.% V alloy which has been annealed at 846 °C and cooled down at 10 °C/min in primary vacuum in the high temperature HTK 1200 Anton Paar chamber was manually polished with an ESCIL silicon carbide abrasive disc (1200 grit). The polishing was stopped when the grey–black layer was totally removed. In Fig. 6, the X-ray diffraction pattern collected at room temperature after $a \approx -0.04$ mm in-depth polishing of the surface confirms the absence of the V_2O_3 phase. The elemental composition was then checked by EDX analysis at 10 randomly selected point locations on the surface of the polished sample. The vanadium content was around 11.2 at.% V, which is in good agreement with the nominal composition of the alloy. In addition, EDX cartographies in Fig. 6 reveals that the platinum and vanadium are homogeneously distributed in the sample. No effect of the annealing in primary vacuum on the bulk composition of the alloy has therefore been noticed. The X-ray diffraction pattern also shows that the disordered cubic phase existing at 846 °C, above the order/disorder transition temperature at 810 ± 10 °C [11], can be retained within the bulk as a single phase by cooling down at 10 °C/min the primary vacuum-annealed Pt–11.1 at.% V alloy. In absence of regions richer in vanadium or in platinum resulting from element segregations within the bulk of the sample, one have to conclude that the force driving the vanadium depletion is its oxidation when the surface of the alloy is exposed to low O_2 partial pressure atmosphere. In the light of what we observed in the current study, the full ordering of vanadium in the Pt–11.1 at.% V alloy near the surface appears as frustrated by its continuous oxidation. Mechanical cold working is known to generate structural metastability or instability principally by increasing the density of extended imperfections (dislocations and interfaces) in the system. These extrinsic imperfections might greatly exacerbate the surface instability of the Pt–11.1 at.% V alloy with respect to oxidation.

Nxumalo and Lang [11] have observed by TEM that small and isolated domains having the ordered tetragonal Pt_8V structure precipitate within the cubic disordered matrix when a 300 µm thick cold-rolled Pt–11.1 at.% V alloy was annealed in the range 300–800 °C. No significant increase in size of the ordered domains has been observed even after long annealing times at 400 °C (2736 h) and 600 °C (720 h). One can wonder whether the long exposure to the low O_2 partial pressure existing in argon could also involve a partial and irreversible segregation of vanadium oxide onto the surface of argon annealed Pt–11.1 at.% V alloy, thus giving the clue of the incomplete disorder/order phase transformation reported by Nxumalo et al. It is noteworthy that the TEM analyses performed by Nxumalo and Lang [11] on argon annealed Pt–11.1 at.% V specimens require the ion polishing of the specimen in order to get an electron transparent area. Since material is sputtered from the specimen during the process, the possible trace of vanadium oxide onto the surface of the alloy exposed to argon is therefore removed. To draw a firm conclusion on this point, the

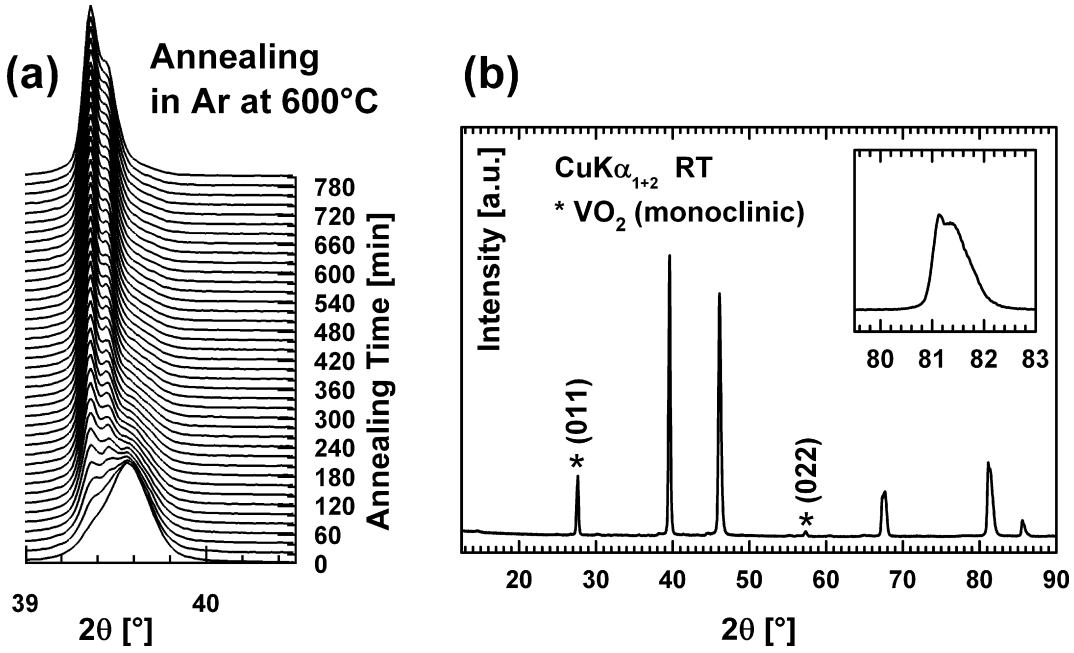

Fig. 7. (a) Appearance with the annealing time of the $(1\,1\,1)_{FCC}$ X-ray diffraction peak of the vanadium-depleted Pt phase (face cubic centred unit cell) when the cold-rolled Pt–11.1 at.% V alloy is annealed at 600 °C in flowing argon atmosphere. (b) Room temperature X-ray diffraction pattern of the Pt–11.1 at.% V alloy after being annealed at 600 °C for 800 min and cooled down at 10 °C/min in argon.

effect of isothermal annealing at 600 °C (corrected temperature) on a raw Pt–11.1 at.% V alloy in flowing argon atmosphere was carried out by *in situ* temperature-controlled X-ray diffraction. The evolution with time of X-ray diffraction patterns recorded at 600 °C is displayed in Fig. 7a. In the (39–40.5°) range, a small shoulder is clearly detected, at $t = 0$ min, on the low scattering angle side of the strong $(3\,0\,1)_{BCT}$ diffraction peak of the tetragonal Pt_8V phase. The position in 2θ of this shoulder corresponds to the one of the $(1\,1\,1)_{FCC}$ cubic peak attributed to the vanadium-depleted (almost pure) Pt phase in the pattern collected on the primary vacuum annealed Pt–11.1 at.% V alloy (Fig. 2b). This $(1\,1\,1)_{FCC}$ peak rapidly grows in intensity with increasing the annealing time without any appearance of diffraction peaks of the sesquioxide V_2O_3 in the (28.5–34.5°) range (not shown in Fig. 7). After isothermal annealing at 600 °C and cooling down to room temperature at 10 °C/min in flowing argon atmosphere, the whole surface of the sample has a light blue tint, thus indicating that an oxidation also takes place. In order to determine the nature of the oxide formed, an X-ray diffraction pattern was collected in the large (12.5–90°) scattering angle range with a 0.0167° step over 125 min. This pattern displayed in Fig. 7b shows an intense peak at $2\theta \approx 27.6°$ and a weaker one at $2\theta \approx 57.3°$ in addition to the peaks ascribed to the mixture of cubic and tetragonal phases (see in insert of Fig. 7b the overlapping of peaks in the (79.5–83°) range). A good match with the monoclinic low temperature form of VO_2 (space group no. 14 $P2_1/c$, PDF 00-043-1051 [27]) is found. This result shows that the coexistence of a cubic phase and of the tetragonal ordered Pt_8V phase reported by Nxumalo and Lang [11] after an annealing of a cold-worked Pt–11.1 at.% V alloy at 600 °C in flowing argon atmosphere has the same origin to the one observed for a primary vacuum annealed specimen: a segregation of a vanadium oxide overlayer (V_2O_3 or VO_2 depending on the O_2 partial pressure) enriching the subsurface region of the alloy in Pt.

Bardi and Ross [30] have carried out a thorough study of the oxidation process taking place at the surface of a Pt_3Ti single crystal annealed at different oxygen partial pressure and temperatures. Above 325 °C, titanium starts segregating from the bulk of the alloy to the surface to form a layer of titanium oxide, thus progressively depleting the subsurface region of the alloy in Ti. The binary Pt_3Ti alloy adopts the ordered Cu_3Au type-structure in which titanium atoms reside only at the corners of the primitive cubic cell. The ordering of such oxophilic atoms in the structure is likely to increase the number of active site at the surface of the alloy for the dry oxidation. It must be remembered that when the ordered Pt_8V phase appears above 448 °C, concomitantly the subsurface region of the Pt–11.1 at.% V alloy starts depleting in vanadium due to its oxidation. This clearly points out that both ordering and oxidation phenomena are correlated and explains why the Pt–11.1 at.% V alloy behaves the same way as Pt_3Ti in oxidizing conditions.

4. Conclusion

In order to gain better insight into the incomplete disorder/order phase transition in cold-rolled Pt–11.1 at.% V alloy, temperature-controlled X-ray diffraction performed in primary vacuum was used to determine the nature of the phases involved in this process. Upon heating above 450 °C, an ordering of vanadium atoms in the Pt–11.1 at.% V alloy leads to the appearance of a tetragonal Pt_8Ti prototype phase. Concomitantly, vanadium atoms at the surface of the ordered alloy are slowly oxidized into V_2O_3 corundum type phase by the low oxygen partial pressure existing in primary vacuum. This segregation of vanadium oxide onto the surface depleting the subsurface region in vanadium, an almost pure Pt cubic phase grows at the V_2O_3-ordered Pt_8V alloy interface with increasing the temperature. If the alloying of platinum with oxophilic atoms can enhance its hardness through a partial or complete disorder/order transformation, the surface instability of the alloy with respect to oxidation can also increase with the ordering of such alloying element.

Acknowledgements

The authors acknowledge the financial support from the CNRS-France and the NRF-South Africa Research Collaboration Programme. The authors are grateful to Cyrille GALVEN (LdOF) for his technical assistance with SEM measurements.

References

[1] D.R. Askerland, The Science and Engineering of Materials, 3rd ed., Stanely Thornes Ltd., 1996.
[2] K.M. Jackson, C.I. Lang, CIMM Conference, UCT, October, 2004.
[3] K.M. Jackson, M.P. Nzula, S. Nxumalo, C.I. Lang, Integrative and Interdisciplinary Aspects of Intermetallics 842 (2005) 497.
[4] M. Carelse, Investigation of the hardening behaviour and ordering transformation in Pt 14 at% Cu, Masters Thesis, UCT, 2005.
[5] E.A. Burke, C.M. Jimenez, L.F. Lowe, Phyical Review 141 (2) (1966) 629.
[6] C.J. Smithells, E.A. Bandes, Metals Reference book, 573, 5th ed., Butterworths, London and Boston, 1976, p. 763.
[7] P. Pietrokowsky, Nature 206 (1965) 291.
[8] P. Krautwasser, S. Bhan, K. Schubert, Z. Metallk. 59 (1968) 724.
[9] D. Schryvers, J. van Landuyt, S. Amelinckx, Materials Research Bulletin 18 (11) (1983) 1369.
[10] D. Schryvers, S. Amelinckx, Acta Metallurgica 34 (1) (1986) 43.
[11] S. Nxumalo, C.I. Lang, Journal of Alloys and Compounds 425 (2006) 181.
[12] M.P. Nzula, C.I. Lang, D.J.H. Cockayne, Journal of Alloys and Compounds 420 (2006) 165.
[13] S. Nxumalo, M.P. Nzula, C.I. Lang, Materials Science and Engineering A 445–446 (2007) 336.
[14] W.E. Quist, C.J. van der Wekken, R. Taggart, D.H. Polonis, Transactions of the Metal Society of AIME 245 (1969) 345.
[15] J.M. Larson, R. Taggart, D.H. Polonis, Metallurgical and Materials Transactions B 1 (2) (1970) 485.
[16] H.A. Moreen, R. Taggart, D.H. Polonis, Journal of Materials Science 6 (12) (1971) 1425.
[17] M.S. Mostafa, A.J. Ardell, Materials Letters 6 (3) (1987) 67.
[18] J. Cheng, M.S. Mostafa, A.J. Ardell, Journal of Less Common Metals 143 (1–2) (1988) 251.
[19] L. Weaver, A.J. Ardell, Scripta Metallurgica 14 (7) (1980) 765.
[20] J. Cheng, A.J. Ardell, Acta Metallurgica 37 (7) (1989) 1891.
[21] A. Gibaud, M. Topić, G. Corbel, C.I. Lang, Journal of Alloys and Compounds 484 (2009) 168.
[22] E.C. Bain, Transactions AIME 70 (1924) 25.
[23] G. Corbel, S. Mestiri, P. Lacorre, Solid State Sciences 7 (2005) 1216.
[24] J. Rodriguez Carvajal, Physica B 192 (1993) 55.
[25] P.-E. Werner, L. Ericksson, J. Westdahl, Journal of Applied Crystallography 18 (5) (1985) 367.
[26] P.M. De Wolff, Journal of Applied Crystallography 1 (2) (1968) 108; G.S. Smith, R.L. Snyder, Journal of Applied Crystallography 12 (1) (1979) 60.
[27] In PDF−4+2009, The International Centre for Diffraction Data (ICDD), 12 Campus Boulevard, Newtown Square, Pennsylvania 19073-3273, USA.
[28] R.J.H. Clark, Comprehensive Inorganic Chemistry, vol. 3, Pergamon Press Ltd, 1973 (pp. 491–551).
[29] V. Grajewski, H.H. Uchida, E. Fromm, Thin Solid Films 193–194 (1990) 990.
[30] U. Bardi, P.N. Ross, Journal of Vacuum Science and Technology A 2 (4) (1984) 1461.